The International Journal of Advanced Manufacturing Technology (2018) 97:4157–4166
https://doi.org/10.1007/s00170-018-2153-0

ORIGINAL ARTICLE

Development of a shape memory alloy actuator using generative manufacturing

Christian Spindler[1] · Daniel Juhre[2]

Received: 21 August 2017 / Accepted: 8 May 2018 / Published online: 8 June 2018

Abstract
A Nitinol hydraulic bellows actuator for the application in minimally invasive surgeries (MIS) has been designed and manufactured. Such application required the actuator to be elastically deformable. This paper explains how the actuator geometry is optimized for large deformations and shows the feasibility of an actuator manufactured by selective laser melting (SLM). Four different shapes were virtually tested using finite element analyses (FEA). Furthermore, multiple samples of the bellows actuator with a U-shaped deformation zone were simulated and manufactured. A test rig was developed to measure deformation and achievable force. Physical tests showed a sufficient performance of the actuator for typical applications in minimal invasive surgery. Technical challenges and potential solutions on the current state of development are discussed.

Keywords Hydraulics · Actuator · Selective laser melting · Shape memory alloy · Bellows · Minimally invasive surgery

1 Introduction

For the handling of tissue during surgery, pinch forces up to 5.6 N are necessary [1]. Taking into account mechanical transmission ratios [2], the actuator force necessary becomes approximately 22 N. This fact, together with the demand for small rod-like dimensions (with a diameter of 5 or 10 mm for instruments) in minimally invasive surgery, limits the types of actuators used in this medical discipline [3].

Hydraulic actuators could meet these requirements [2, 4]. However, hydraulic cylinder-piston actuators lack flexibility and leak tightness. Flexible, hermetically sealed actuators presented in previous studies [4–6] generate only small forces because of an applied pressure below 0.55 MPa [6].

The ideal drive for instruments in minimally invasive surgeries is hermetically sealed and flexible. Moreover, it should provide a minimum force of 22 N and its shape should be rod-like with a maximum outside diameter of 5 mm. To satisfy these requirements, a flexible hydraulic actuator with a strong but flexible shell to withstand high pressures but to sustain large deformations should be developed. Theoretically, a bellows-shaped actuator could be able to satisfy these requirements [7].

Nitinol fulfills the core requirements with regard to the material properties. It is an alloy of nickel (Ni) and titanium (Ti) which exhibits shape memory properties. This means that the material's original shape can be restored after deformation beyond its elastic range [8]. This is due to the effect of a diffusionless phase transformation. Nitinol appears in two phases, austenite and martensite. At high temperatures (above the austenitic start temperature A_s), the meta-stable phase is austenitic. By increasing the stress, it transforms into martensite. When the mechanical stress is released, it transforms back to austenite and the original shape is recovered. This effect is called pseudoelasticity. Below the martensite start temperature M_s the martensitic phase in a twinned state is dominant. By increasing the stress, the twinned martensite is oriented and it deforms plastically without generating dislocations. Increasing working temperature (above A_s), it transforms back to austenite, turning back to original shape [9]. The presence of the pseudoelastic or pseudoplastic state is affected by working temperature, alloy composition, heat treatment, and microstructure of the material [8]. The proposed actuator is manufactured in such a way that the pseudoelasticity can be utilized (see also

✉ Christian Spindler
Christian.spindler@ipa.fraunhofer.de

[1] Fraunhofer Institute for Manufacturing Engineering and Automation, Mannheim, Germany

[2] Otto von Guericke University, Magdeburg, Germany

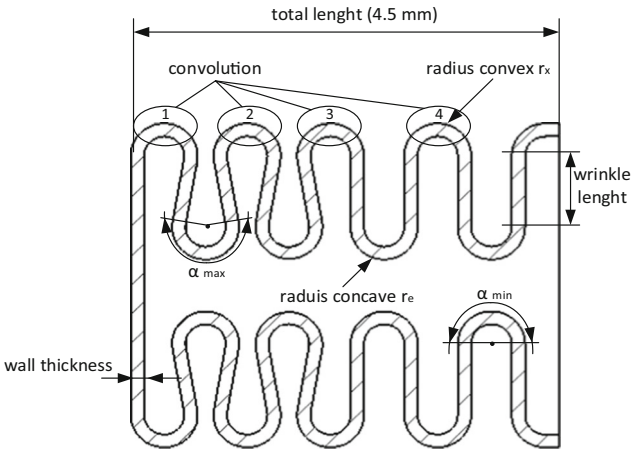

Fig. 1 General bellows parameters

Section 2.3). Nitinol achieves a reversible strain of 8%, a good functional stability with a yield stress up to 1120 MPa and a tensile strength up to 1200 MPa [8]. Additionally, Nitinol has good corrosion resistance and biocompatibility and is already used for various medical applications [8].

One of the main challenges of using Nitinol for semi-finished parts or final components is that the manufacturing requires considerable effort to achieve the particular properties of the material [8]. In addition, the bellows actuator has a complex hollow shape with convolutions and small dimensions.

Haberland [8] described a complete process for selective laser melting (SLM) of Nitinol. In this study, the shape memory properties of additively manufactured Nitinol were verified in pressure tests using cuboid samples (10 mm × 10 mm × 6 mm) [8]. Krishna et al. manufactured and tested porous Nitinol alloy samples with a cylindrical shape, a diameter of 7 mm, and a length of 15 mm. They measured maximum strains of 4 to 6% [10]. Other studies [6] used finite element analysis (FEA) simulations to characterize/optimize/develop/design polymer bellows. The results were compared to experimental data from micro-bellows actuators manufactured using micro-stereolithography and are, measured in elastic range, in good agreement. There was a linear relationship between displacement and input pressure which was shown in three different experiments [6].

The goal of this work is to optimize a bellows design for SLM and validate that SLM is a feasible manufacturing method for such an actuator. The optimization is achieved by FEA and the validation through physical testing. This paper focusses on a bellows actuator with an outside diameter of 5 mm providing a relative strain of 1.2% and forces up to 24 N. For its realization, fine structures and a wall thickness of 100 μm are necessary. Moreover, the radius profile and hollow form require a complex shape which is difficult to manufacture. To generate large forces and large deformations, high material strength and elasticity are necessary, too. As stated previously, Nitinol fulfills these requirements. However, a suitable manufacturing process needs to be found and optimized.

2 Materials and methods

This section describes the design, manufacturing, and evaluation process which is necessary to develop the bellows actuator.

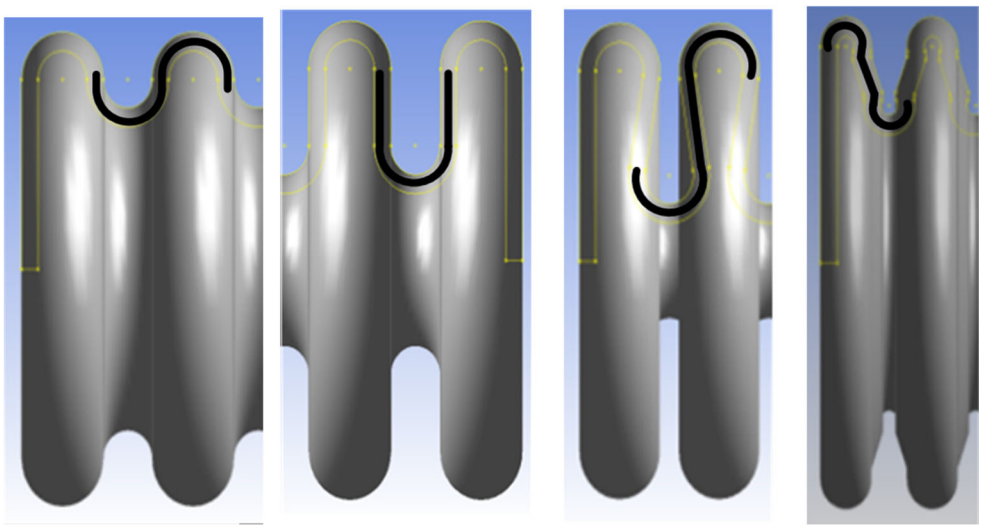

Fig. 2 Different bellows shapes have been considered in this study. **a** S-structure. **b** U-structure. **c** J-structure. **d** Solid joint structure

Table 1 Parameters of bellows shapes with total length of 4.5 mm

Used shape	S-structure	U-structure	J-structure	Solid joint
Radius r [mm]	0.25	0.25	0.25	0.15
Wall thickness [mm]	0.1	0.1	0.1	0.1
Number of convolutions	4	4	7	7

2.1 Design of a promising actuator shape

To design an actuator, the general bellows parameters were examined [Fig. 1]. The convex radius and the concave radius of the bellows actuator have the same value and are kept constant in this investigation $r = r_x = r_e$. Furthermore, the radius angle α was selected to be the same for convex and concave radii. The number of convolutions was counted as shown in Fig. 1. To ensure comparability, the same total length of $l = 4.5$ mm was set for each bellows shape. To fulfill this, the number of convolutions had to be adjusted depending on the chosen shape.

To obtain an actuator with maximum deformation in the axial direction and minimum stress, the following four bellows shapes were designed and examined. In its typical application as a protective cover, in which deformations are needed, bellows occur in S-structure [Fig. 2a], U-structure [Fig. 2b], and J-structure [Fig. 2c]. Taking inspiration from solid joints in instrument tips of minimally invasive instruments, in which deformations based on elastic bending occur, a solid joint structure [Fig. 2d] was chosen as a fourth option.

The following overview clarifies the differences between the individual structures:

S-structure [compare Fig. 1 and Fig. 2a]

The shape created when "convex" and "concave radius" follow directly each with a "radius angle" α of 180°.

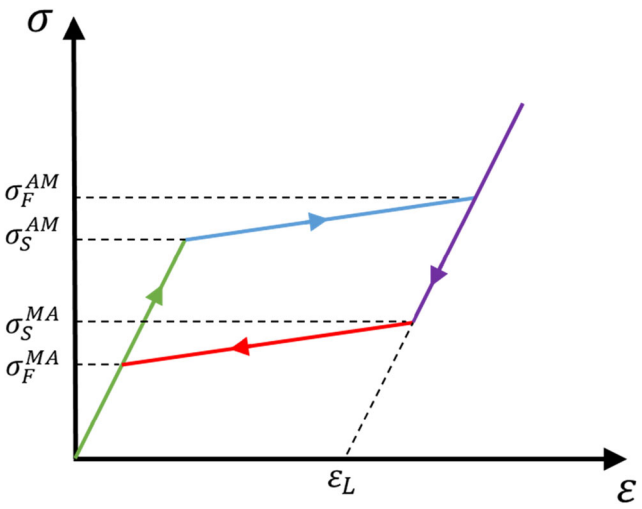

Fig. 3 Stress-strain relation in pseudoelasticity

U-structure [compare Fig. 1 and Fig. 2b]

The shape created when there is a distance between the convex and concave radius. This straight line is named "wrinkle length." Each arc has a radius angle α of 180°.

J-structure [compare Fig. 1 and Fig. 2c]

This structure has also a wrinkle between the convex and concave radius. However, the radius angle α is between 180° and 221° which results in an undercut in bellows geometry.

Solid joint structure [compare Fig. 1 and Fig. 2 d]

For the solid joint structure, the radius angle α is 180° and there is a wrinkle between convex and concave radius. The convex and concave radii are not connected directly to the wrinkle. They are connected by solid joints, i.e., kink areas with smaller wall thicknesses allowing for higher local flexibility.

The shapes were simulated by using the commercial FEA tool Ansys, with the parameters in Table 1.

2.2 FEA analysis

The pseudoelastic characteristics of Nitinol were modeled using a material model which included the simplified stress-strain relationship of shape memory alloys as shown in Fig. 3. Here, the green line signifies the linear elastic response of the material due to loading until the specific stress level σ_S^{AM}. At this level, the phase transformation from austenite to martensite is initiated and coincides with a small increase of stress with regard to the strain (blue line). At the stress level σ_F^{AM}, which correlates with the transformation strain ε_L , the phase

Table 2 Used material parameters for Nitinol shape memory effect

Initial stress for phase transformation -Austenite to martensite—$\sigma^{AM}{}_S$ [MPa]	520
End stress for phase transformation -Austenite to martensite—$\sigma^{AM}{}_F$ [MPa]	600
Initial stress for phase transformation -Martensite to austenite—$\sigma^{MA}{}_S$ [MPa]	300
End stress for phase transformation -Martensite to austenite—$\sigma^{MA}{}_F$ [MPa]	200
Maximum transformation strain ε	0.07

Table 3 Comparison of maximum equivalent stress, maximum deformation, strain, and a qualitative rating for fabricability for different shapes with total length of 4.5 mm at a pressure of 10 MPa

Examined shape	S-structure	J-structure	U-structure	Solid joint
Stress [MPa]	668.27	752.96	688.04	699.03
Total stain [%]	2.2	14.9	6	4.4
Deformation [mm]	0.1	0.67	0.27	0.2
Manufacturing rating [1 = good, 3 = bad]	1	2	1	3

transformation is terminated and hence, the material response is assumed to be again linear elastic (purple line). During unloading, reaching a lower stress level σ_S^{MA}, the retransformation starts and is ending at σ_F^{MA} (red line). Finally, after the complete loading cycle, stress and strain have been fully recovered. It has to be considered that this model is quite popular but also simple, since more complex occurrences (like, e.g., post-plasticity or small amounts of remaining strains due to fatigue) cannot be taken into account. The necessary material parameters are summarized in Table 2.

All aforementioned structures were analyzed in FEA simulations. A fixed bearing boundary condition was used for the deformation region [Fig. 5]. A pressure of 10 MPa at the inner surface of the bellows was applied. Table 3 shows results of a static structural analysis of this system and an ease-of-manufacturing rating.

The J-structure shows the maximal deformations, whereas the S-structure was the geometry with least maximum equivalent stress.

To compare the simulations to physical tests, a bellows actuator was designed and manufactured [Fig. 4]. The U-structure was chosen, because this geometry promised a good compromise between low stress and high deformations. Also, at this geometry, the radius angle α is 180° and does not include any undercut, rendering the manufacturing process much easier than for the J-structure. The designed bellows actuator comprises a deformation region in the middle and two joints (one at every end) [Fig. 5]. The union joint has a conical axial drilling of 0.78 to 0.9 mm to connect a pressure supply tube. The outside diameter is 3.02 mm with two pins (0.5 mm) at each side for connecting to the test rig. The auxiliary joint has an axial drilling of 1.0 mm. Its outside diameter is 2.0 mm and has a drilling of 0.50 mm for connecting to the test rig. The change in wall thickness in these three zones is kept low: In the deformation region, it is fixed to 100 μm and in the joint regions, it ranges from 100 to 200 μm. The total structure length is 16.5 mm.

The actuator was pressurized with 10 MPa. The maximum of equivalent stress increased to 737.58 MPa at the convex radius (red) and was at minimum at joint region (blue) of bellows actuator [Fig. 6a, b].

The deformation was directly proportional to the applied pressure. At 10 MPa, the deformation was 1.53 mm which corresponds to 9.2% global strain. Figure 7 highlights the simulation results for the pressure range up to 1.29 MPa accessible by the physical tests described later in Section 2.5. Here, we find a total axial deformation of 0.26 mm and a global strain of 1.57%.

2.3 Fabrication of a prototype actuator

Nitinol with a composition of 55.97 wt% Ni and 44.03 wt% Ti was used. The A_s temperature was in a range of − 24 to − 12 °C and the A_f temperature in a range of − 11 to + 1 °C. A Nitinol bar was processed into powder by electrode induction-melting gas atomization process (EIGA) and fractionated by sieving. Only the 10- to 30-μm fraction was selected due to the small structure size in our SLM process. To increase flowability, particles smaller than 10 μm were removed by

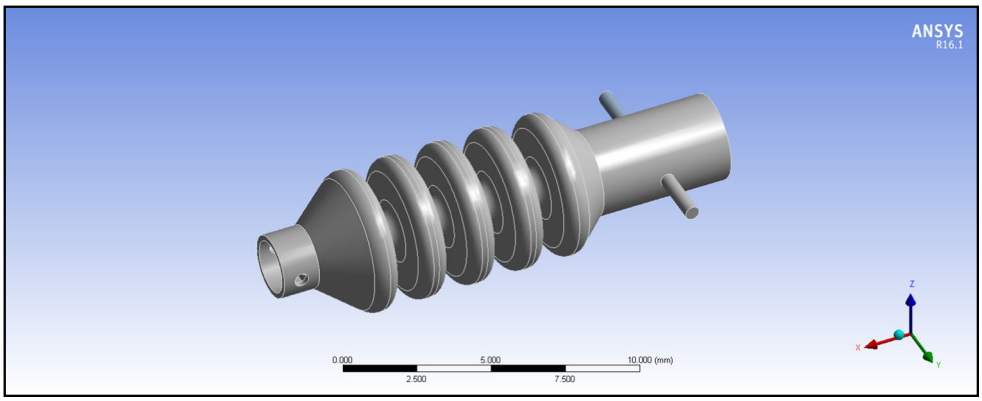

Fig. 4 In Ansys designed bellows actuator with U-structure

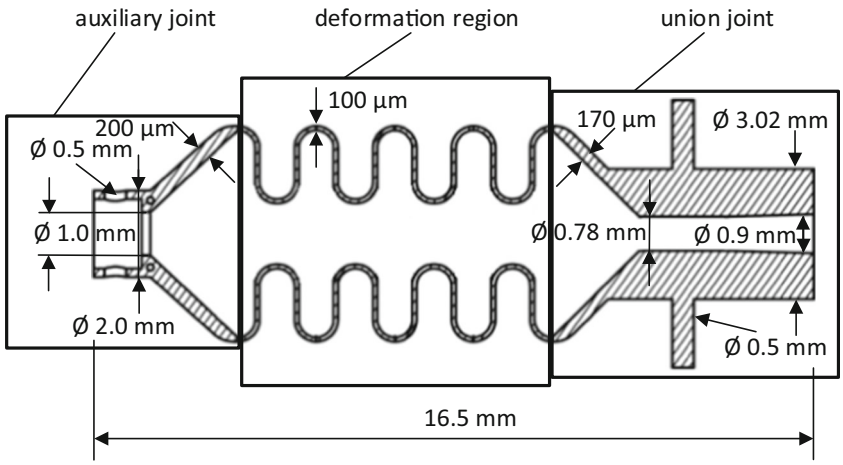

Fig. 5 Schematic figure of bellows actuator with U-structure

powder air separation. The powder was checked for contamination by carbon, oxygen, and nitrogen described in [8]. The processed and analyzed material was then used as raw material for the SLM process.

Fifteen bellows actuators were manufactured using SLM. Haberland [8] and Bormann et al. [12] describe the manufacturing in general. This process was carried out in an inactive Ar atmosphere and on a Nitinol substrate plate using a Realiser SLM-50 system.

Support structures were removed by grinding. Afterwards, a heat treatment was necessary to arrange structural conditions after the remelting process. During the heat treatment, the Nitinol actuator was placed in an airtight glass case together with a titanium getter preventing physical contact of Nitinol and titanium. The getter is used to absorb residual oxygen to prevent oxidation of the actuator material. Heat treatment was processed in a vacuum oven. As described in [8], solution annealing at 950 °C for 5.5 h, rapid cooling, aging at 350 °C for 24 h, and again rapid cooling followed the heat treatment.

To seal the pores (to prevent leakage), a parylene coating with a thickness of 5.5 µm was applied. The union joint of the bellows actuator was glued to a polyimide tube with an outer diameter of 0.637 mm and an inner diameter of 0.513 mm. The tube was then connected to a water-filled syringe. The actuator was filled completely and the auxiliary joint was sealed. Pressure was applied by a syringe pump to check tightness.

2.4 Experimental setup

The test setup is shown in the following drawing [Fig. 8].

A force sensor and a displacement sensor were connected to the bearings. Adjusting elements were integrated to fix the movable bearing in place for the force measurements. The bellows were coupled in the joint regions working like a bayonet catch. The hydraulic supply lines for the bellows and test rig were filled with water, degassed, and coupled. Pressure and flow rate were automatically controlled by a computer program which also recorded the measured force, displacement, and pressure. The displacement was assumed to be equivalent to the absolute deformation of the actuator.

2.5 Deformation test

Deformation tests were performed to check longitudinal deformation of the bellows actuator by increasing the pressure. Water flow rates of 1, 3, and 5 µl/s were applied. The maximum achievable pressure in these experiments was 1.29 MPa. After reaching maximum pressure and deformation, the pressure was released immediately.

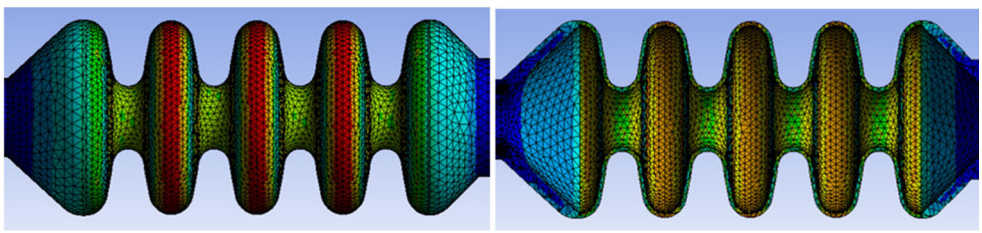

a) Outside surface b) Cut section

Fig. 6 Equivalent stress of bellows actuator with U-structure simulated in Ansys. **a** Outside surface. **b** Cut section

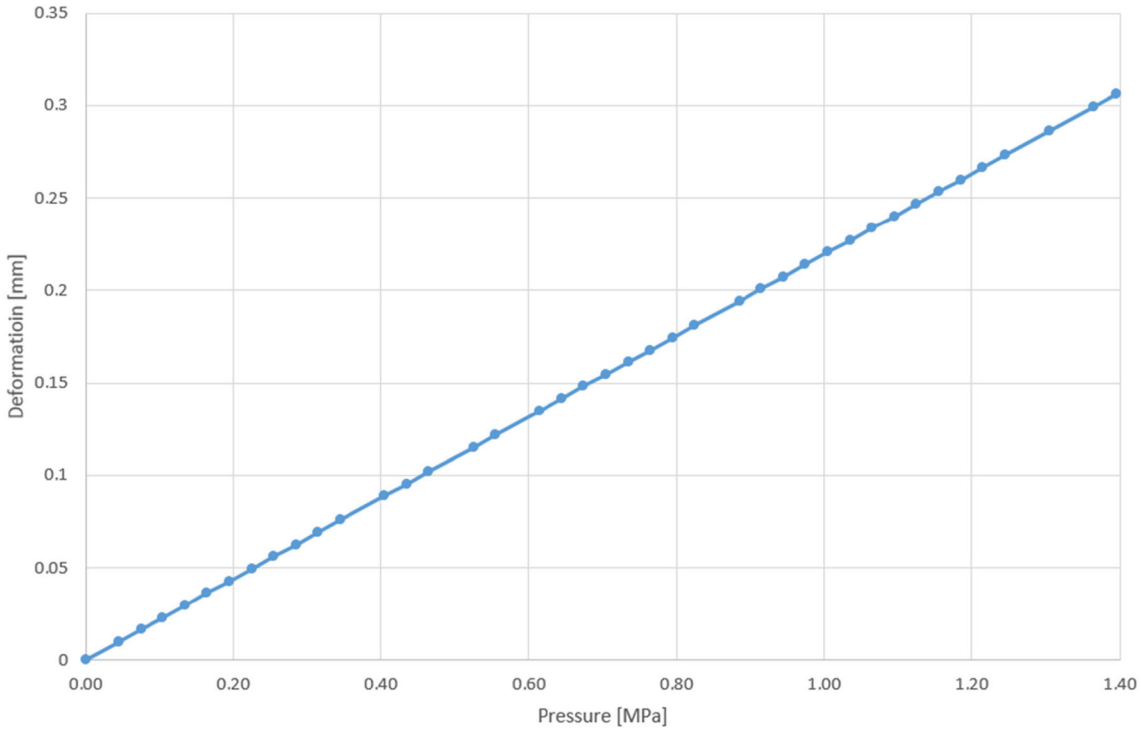

Fig. 7 Simulated deformation of U-structure bellows actuator as function of pressure

The adjusting elements were unlocked. The movable bearing could move freely during the entire test. Table 4 shows the measured results.

2.6 Force test

To determine the maximum achievable force in the axial direction by an increasing pressure, a force test has been performed. Moreover, the stability of the material was observed. These tests were performed at a flow rate of 5 μl/s. The maximum pressure loads tested were 1.5 and 5.5 MPa. After reaching the maximum, the pressure was released immediately. To prevent actuator deformation, the movable bearing was fixed in its initial state. The generated force at applied pressure and flow rate were measured and are shown in Fig. 10.

3 Results

3.1 Physical experiments

3.1.1 Deformation test

Table 4 shows the absolute deformation of a bellows actuator with a total length of 16.5 mm. It showed that the maximum achieved pressure depended on the input flow rate. Deformation and pressure demonstrated a linear correlation

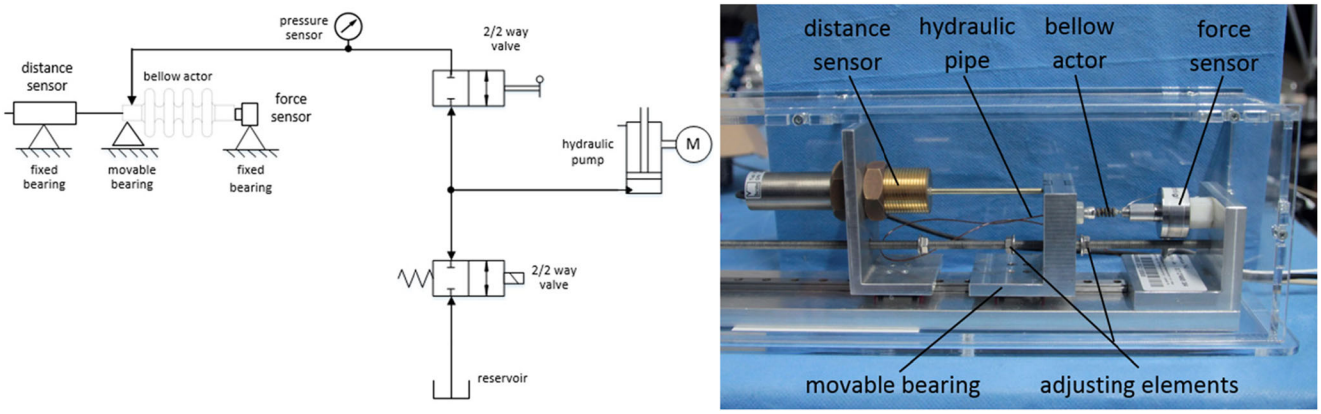

Fig. 8 Schematic hydraulic circuit for actuator characterization and physical setup for force and deformation tests

Table 4 Deformation of 16.5-mm length bellows actuator in dependence of flow rate and pressure

Test number	Flow rate [µl/s]	Maximum pressure [MPa]	Deformation [mm]
1	1	0.94	0.14
2	3	1.22	0.19
3	5	1.29	0.20
4	5	1.17	0.17

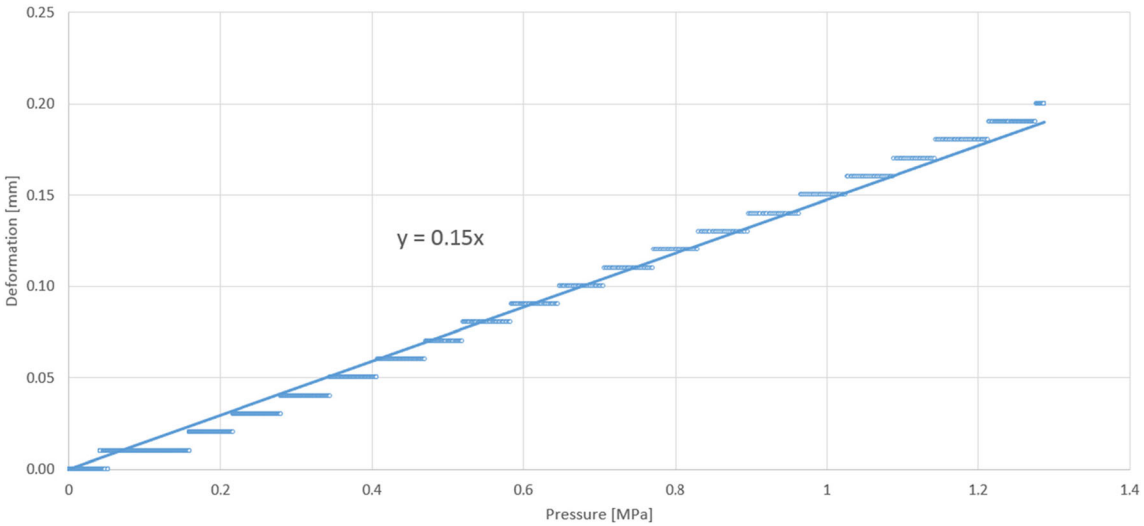

Fig. 9 Measured values of test number 4 and trendline of deformation of 16.5-mm length bellows actuator as a function of pressure

as shown in Fig. 9. Approximately 3000 data points were recorded. A flow rate between 1 and 5 µl/s was necessary to compensate liquid leaking and stabilize the pressure applied to the actuator. Necessary flow rates varied for individual experiments and are given in Table 4. As a result of the manufacturing process, only one bellows actuator could be tested. Leaking appeared at the joint regions, as well as at areas of convex and concave radius in the deformation region. Outflowing drops were visible. Nevertheless, the actuator responds comprehensibly. After pressure release, the actuator did not return to its original length. Thus, the length of the actuator was manually readjusted to its initial length of 16.5 mm for subsequent tests. A global strain of 1.2% was measured for the maximum pressure of approximately

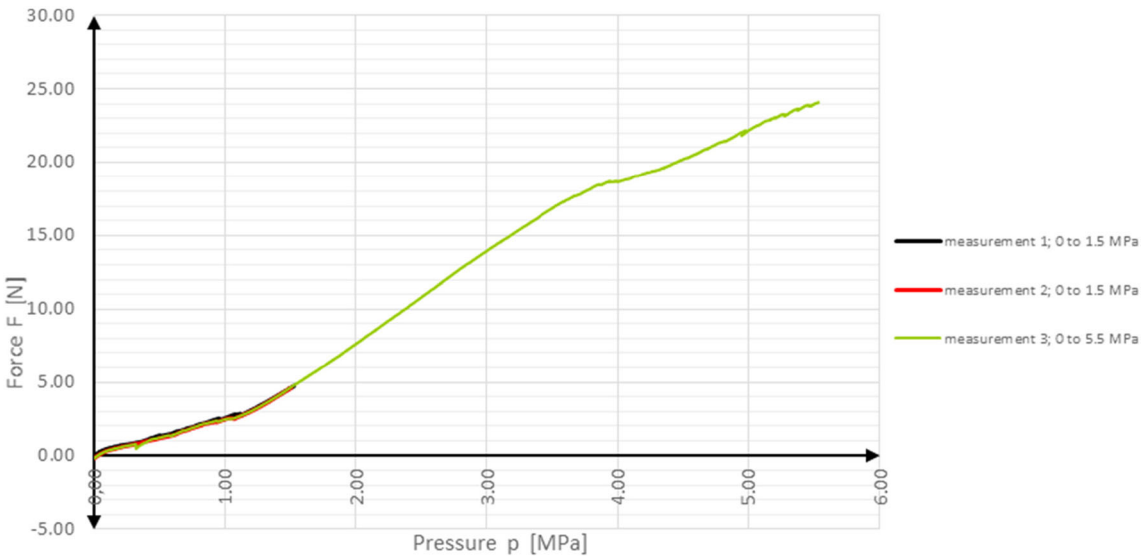

Fig. 10 Three measurements show force as a function of pressure at flow rate of 5 µl/s

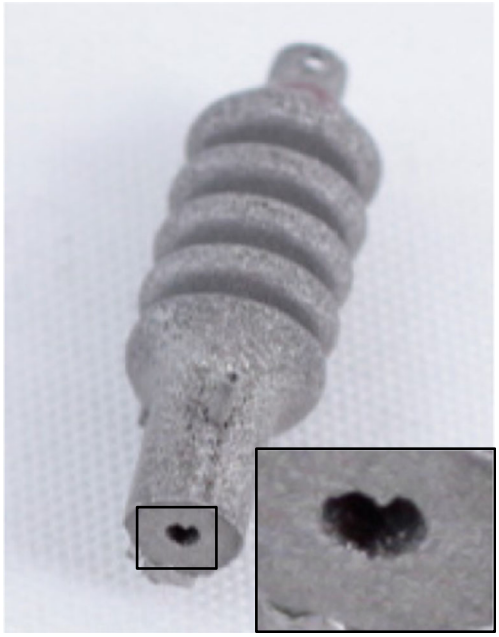

Fig. 11 Bellows actuator with oval-shaped hole in union joint

1.29 MPa. The deformation, which is shown in Fig. 9, depends linearly on pressure.

3.1.2 Force test

Figure 10 illustrates the results for three measurements of force as a function of pressure.

The measurement to 1.5 MPa was done twice. The second was to a pressure of $p_{max} = 5.5$ MPa and a flow rate of 5 μl/s. A nearly linear behavior can be observed up to 4.7 N at 1.1 MPa. Between the measurements 1 and 2, only insignificant differences have been found. At the measurement to maximum pressure $p_{max} = 5.5$ MPa, a force $F_{max} = 24$ N was measured. The relationship between pressure and force of measurement 3 was similar to the measurements 1 and 2 up to 1.5 MPa. Between 1.5 and 4.0 MPa, a stronger but still linear increase of force with pressure was observed. In the force test, leaking was observed by visible drops, however, less than in the deformation test. Despite leaking, the actuator reacts comprehensible.

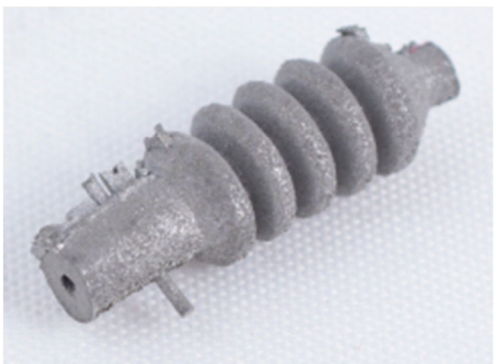

Fig. 12 Bellows actuator produced by selective laser melting

3.1.3 Optical evaluation of bellows actuator manufacturing

Fifteen bellows actuators were manufactured in three processes with the same machine parameters. However, parameters which are not precisely adjustable, such as the powder application and the distribution of the bellows actuators in the machine, did influence the individual quality of the bellows actuators.

The axial hole was continuous through the linking regions and the deformation region. Although the support structures had been removed, there were some residues on the outer surface. No cracks or broken out material could be observed. The auxiliary joint had a round shape. Wall thickness and holes for connection were produced as foreseen. The hole at the union joint for tube connection was smaller than expected. The hole had an oval shape at ceiling because of "stalactites" [Fig. 11]. The surface was porous and especially in deformation region very thin. There were deviations between the CAD modeled and fabricated geometries. Depending on the region of interest, a dimensional stability of 0.33 to 2.91% was achieved for the best fabrication batch, when compared to the designed CAD model. Figure 12 shows one of those actuators. However, not all bellows actuators had this appearance. Some samples were afflicted with residual support structures and deformed in the axial direction. Cracks and holes were observed on the bellows' surface area. These errors are highlighted in Fig. 13. At the end wall of one actuator were cracks starting from the hole and reaching almost to the outside wall [Fig. 14]. The ceilings of the holes—observed in direction of manufacturing—had stalactites which resulted in an oval shape. The chemical analysis showed a contamination of 0.0280 wt% carbon, 0.0450 wt% oxygen, and less than 0.0020 wt% nitrogen. Two bellows actuators were able to

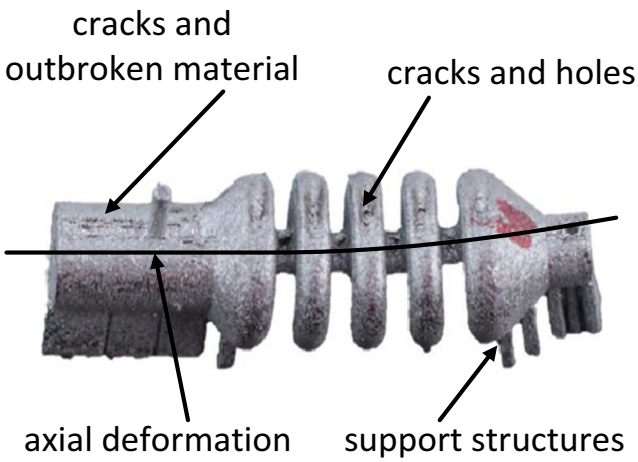

Fig. 13 Bellows actuator with cracks and holes, deformed in axial direction

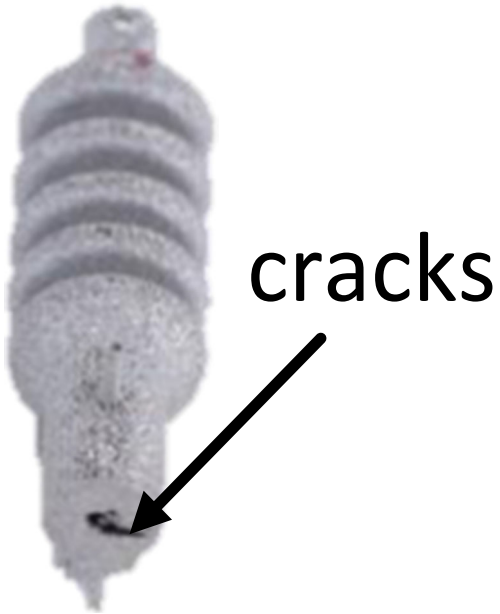

Fig. 14 Bellows actuator with cracks at the end wall

reach a pressure of 0.1 MPa. These could not be used in the "deformation test". The parylene coating shifted this threshold to a pressure of 1.29 MPa in the "deformation test" and to a pressure of 5.5 MPa in the "force test"—with fixed actuator.

4 Discussion

Novel miniature Nitinol bellows actuators were designed, simulated, manufactured, and investigated. The deformations in FEA simulations and physical tests were both linear [Fig. 15]. This was comparable to the results of Hyun-Wook Kang et al. [6] who investigated polymer bellows actuators. Polymer actuators could only be used to a pressure of 0.33 MPa. However, for the high force application, a high-strength material was needed. The simulation results showed a higher increase of deformation in comparison to the physical tests. This was likely caused by the relatively high porosity of the manufactured bellows and differing material properties. The respective material parameters of the physical actuator have not yet been determined. Due to water leakage, during physical deformation tests, a pressure of 1.29 MPa could not be exceeded. Probably, the results will be slightly different for tight bellows, but they will be qualitative in a similar field.

Force tests verified a maximum force of 24 N at 5.5 MPa and a nearly linear relationship between applied pressure and generated force. To drive a minimally invasive instrument, a force of 22 N is necessary [1, 2]; thus, this type of actuator would fulfill this requirement.

To achieve large deformations and greater forces, sealed bellows are recommended. Further investigations to find the leaking hot spots are necessary. For this, the manufacturing process must be investigated. The dimensions of the bellows actuator were very small and the shape was very complex. Thus, it seems that for the dimensions and shapes discussed here are close to the current technical limit of SLM production. The surface of the produced bellows actuator was porous and notably thinned in the deformation region. Vasmsi Krishna et al. [10] observed no permanent deformation of porous Nitinol samples at 2% total strain. After an applied total strain of 4%, a permanent strain of 0.2 to 0.6% was

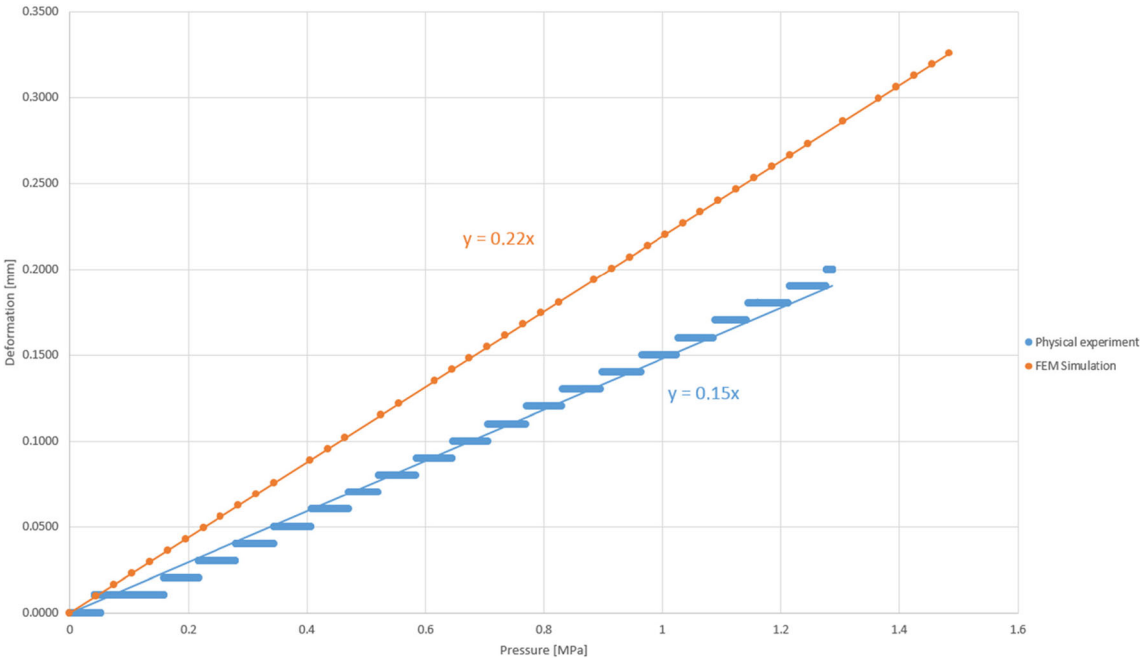

Fig. 15 Comparison of physical deformation and simulated deformation in depending on pressure

measured which is similar to 6% total strain of samples with high density. Thus, porous Nitinol is in principle suitable for bellows actuator applications. However, in the experiments shown here, there were more and bigger pores situated in overhang areas. Some pores were evidently large enough for water to leak through when pressure was applied. Adjustable parameters without changing the SLM machine are the position of bellows in machine and an improved design of the bellows shape. Recommended improvements include supports for the overhangs or a geometry avoiding overhangs. As well, less variation of wall thickness at interfacial between linking region and deformation regions should be helpful. This looks like a solvable issue that can be addressed by recent technological developments.

Contamination of 0.0280 wt% carbon, 0.0450 wt% oxygen, and less than 0.0020 wt% nitrogen was measured. "These impurities can degrade the shape memory effect" [translated from 8]. Oxygen and carbon contamination affect the transformation temperature. Oxygen is known to degrade mechanical properties. The material becomes more brittle and shows an earlier crack initiation. Carbon increases the strength and pseudoelasticity characteristics to higher temperature region. Further, it leads to a reduction of deformability at similar values [11].

5 Conclusion

It was shown that SLM manufacturing for Nitinol in bellows shape is possible. With this type of actuators, high forces and relative displacements can be achieved by pressure application.

Next steps should be to optimize sealing and manufacturing methods. The microstructural condition should be verified by tests to ensure an austenitic structure from the initial load. Moreover, the negative influence of impurity on the pseudoelasticity could be shown. For new powder production, a customized optimized Nitinol alloy in small quantities should be used. Simulations with linear elastic material could be done to compare the improvement and confirm the pseudoelasticity.

This study showed that a bellows actuator with an outside diameter of 5 mm can be used to drive a minimally invasive surgical instrument. In principle, a shape memory alloy is suitable for this application and it can be manufactured by selective laser melting. This is a new actuator with great future potential compared to conventional hydraulic actuators for use in minimal invasive surgery.

Acknowledgements The authors acknowledge the Fraunhofer Institute for Laser Technology (ILT) for the SLM fabrication of the actuator prototypes used in the present study.

References

1. Westebring-van der Putten EP, van den Dobbelsteen JJ, Goossens RHM, Jakimowicz JJ, Dankelman J (2009) Effect of laparoscopic grasper force transmission ratio on grasp control. Surg Endosc 23(4):818–824. https://doi.org/10.1007/s00464-008-0107-6
2. Cuntz T (2015) Untersuchungen zur Eignung mikrohydraulischer Antriebe für die minimal invasive Chirurgie. Dissertation
3. Carus T (2014) Operationsatlas Laparoskopische Chirurgie. Springer
4. de Volder M, Reynaerts D (2010) Pneumatic and hydraulic microactuators: a review. J Micromech Microeng 20(4):43001. https://doi.org/10.1088/0960-1317/20/4/043001
5. Ikuta K, Ichikawa H, Suzuki K et al (2006) Multi-degree of freedom hydraulic pressure driven safety active catheter. In: ICRA '06: Proceedings of the 2006 IEEE International Conference on Robotics and Automation, pp 4161–4166
6. Kang H-W, Lee IH, Cho D-W (2006) Development of a micro-bellows actuator using micro-stereolithography technology. Microelectron Eng 83:1201–1204
7. Spindler C, Kaltenbacher D, Schächtele J (2013) Powerful micro-actuators for (flexible) surgical instrument tips. BMT
8. Haberland C (2012) Additive Verarbeitung von NiTi-Formgedächtniswerkstoffen mittels selective laser melting. Dissertation
9. Van Humbeeck J (2001) Shape memory alloys: a material and a technology. Adv Eng Mater 3:837–850
10. Krishna BV, Bose S, Bandyopadhyay A (2009) Fabrication of porous NiTi shape memory alloy structures using laser engineered net shaping. J Biomed Mater Res 89((2):481–490. https://doi.org/10.1002/jbm.b.31238
11. Krone L (2005) Metal-injection-moulding (MIM) von NiTi Bauteilen mit Formgedächtniseigenschaften. Dissertation
12. Bormann T, Schumacher R, Müller B, Mertmann M, de Wild M (2012) Tailoring selective laser melting process parameters for NiTi implants. J Mater Eng Perform